FREEZING SOLUTIONS OF EQUIVARIANT EVOLUTION EQUATIONS

W.-J. BEYN*, V. THÜMMLER*
FAKULTÄT FÜR MATHEMATIK, UNIVERSITÄT BIELEFELD,
POSTFACH 100131, D-33501 BIELEFELD, GERMANY.

Abstract. In this paper we develop numerical methods for integrating general evolution equations $u_t = F(u), u(0) = u_0$, where F is defined on a dense subspace of some Banach space (generally infinite dimensional) and is equivariant with respect to the action of a finite dimensional (not necessarily compact) Lie group. Such equations typically arise from autonomous PDE's on unbounded domains that are invariant under the action of the Euclidean group or one of its subgroups. In our approach we write the solution $u(t)$ as a composition of the action of a time dependent group element with a 'frozen solution' in the given Banach space. We keep the 'frozen solution' as constant as possible by introducing a set of algebraic constraints (phase conditions) the number of which is given by the dimension of the Lie group. The resulting PDAE (Partial Differential Algebraic Equation) is then solved by combining classical numerical methods, such as restriction to a bounded domain with asymptotic boundary conditions, half-explicit Euler methods in time and finite differences in space. We provide applications to reaction diffusion systems that have traveling wave or spiral solutions in one and two space dimensions.

Key words. General evolution equations, equivariance, Lie groups, partial differential algebraic equations, unbounded domains, asymptotic boundary conditions

AMS subject classifications. 65M99, 35K57

1. Introduction.

We consider the numerical solution of general evolution equations

$$u_t = F(u), \quad u(0) = u_0, \tag{1.1}$$

that are equivariant with respect to the action of a finite-dimensional, not necessarily compact Lie group. Equation (1.1) is considered on a Banach space X where the mapping F has a dense domain. Equivariance means that we have a finite dimensional Lie group G which acts on X via a representation $a : G \mapsto GL(X)$ such that F is equivariant in the sense $F(a(\gamma)v) = a(\gamma)F(v)$ for all $\gamma \in G$ and for all v in the domain of F.

The main application we have in mind are reaction-diffusion systems on unbounded domains $\Omega \subset \mathbb{R}^d$ such as the semilinear system

$$u_t = \Delta u + f(u), \quad x \in \Omega, \quad u(0) = u_0, \tag{1.2}$$

where $u(x,t) \in \mathbb{R}^m$ and $f : \mathbb{R}^m \mapsto \mathbb{R}^m$ is sufficiently smooth. If the domain Ω is invariant with respect to the action of a Lie Group $G \subset GL(\mathbb{R}^d)$ then this induces an equivariance of (1.2) via the action

$$[a(\gamma)v](x) = v(\gamma x), \quad x \in \Omega$$

where v is in some suitable function space. In case $\Omega = \mathbb{R}^d$ equivariance holds with respect to the Euclidean group $G = SE(d)$. Further symmetries may be induced by special equivariance properties of the linear and nonlinear part in (1.2).

*Supported by DFG research group 'Spectral analysis, asymptotic distributions and stochastic dynamics', University of Bielefeld.

Up to now there is a well developed bifurcation theory for equivariant dynamical systems that covers the infinite dimensional case of PDE's and certain aspects of noncompact Lie groups, see the monographs [12],[6]. In particular, we refer to [13], [23] and the remarkable series of papers [10],[28],[29],[11]. One of the underlying ideas in the latter papers is to transform the flow of (1.1) into so called skew product form. One part is orthogonal to the group orbit (of the initial value) and the other part acts within the group orbit and depends upon the position in the orthogonal direction, compare [10]. Combining this decomposition with center manifold reductions (see [28],[29]) leads to a powerful tool for studying equivariant bifurcations in PDE's. In this way, various bifurcations of spiral waves, observed and interpreted in [1],[3], could be put into a mathematically rigorous framework.

In this paper we propose a numerical method for solving the initial value problem that makes use of the equivariance by extending the system (1.1) rather than reducing it as in bifurcation analysis. More precisely, we write the solution $u(t)$ of (1.1) as

$$u(t) = a(\gamma(t))v(t), \tag{1.3}$$

where $\gamma(t) \in G$ and $v(t) \in X$ are to be determined. The extra degrees of freedom $\gamma(t)$ are compensated for by phase conditions

$$\psi(v, \gamma) = 0, \tag{1.4}$$

the number of which is given by the dimension of the Lie group. The resulting system for $(v(t), \gamma(t))$ (see equation (2.18)) is an abstract differential algebraic equation which will be set up and analyzed in some detail in section 2. The choice of phase condition is crucial for our approach since it determines the parametrization of the v-orbits.

In section 2.3 we discuss several choices for the function ψ in (1.4) that are based on minimization or orthogonality principles. In particular, near relative equilibria of (1.1) (i.e. solutions of the form $u(t) = a(\gamma(t))v$) the phase condition should force the v-part of the solution to become stationary. For this reason we will sometimes call $v(t)$ the *frozen solution* and the transformed system the *frozen system*.

Applications to parabolic systems (1.2) in one and two space dimensions will be discussed in sections 2 and 3. The frozen system in this case turns out to be a PDAE (Partial Differential Algebraic Equation) which will be solved in a straightforward manner by a half-explicit Euler method. For numerical computations one has to restrict the infinite to a finite domain and use appropriate boundary conditions. After this truncation the original and the frozen system are no longer equivalent. For example, when a traveling wave (or a drifting spiral) reaches a finite boundary in the given system it will usually die out, while in the frozen system it is expected to become stationary.

In section 3 we will discuss several two-dimensional systems from the literature (e.g. Barkley's spiral system [1],[3], the $\lambda - \omega$-system [18] and the quintic Ginzburg Landau equation [7],[8]) that show rigidly rotating spiral waves. Freezing such waves can be delicate because it depends on the precise choice of phase condition (with or without weighted L^2-norms), the type of numerical discretization (rectangular or polar grid) and on the right choice of the underlying group. Note that a related approach to ours was developed in [5] with the intention to use the side constraint in order to fix the tip of a spiral wave. Also in [2] Barkley mentions the use of a pinning or phase condition in order to compute the spiral wave from a time-independent boundary value problem.

While there have been quite a few numerical bifurcation methods that employ equivariance with respect to compact and mostly discrete groups (see [14, Ch.8] for a recent survey) it seems that equivariance with respect to general Lie groups has not been systematically used for solving equivariant systems numerically. We expect that, apart from the evolution system (1.1), our general approach will also be useful for the numerical bifurcation analysis of relative equilibria and relative periodic orbits.

Note added in proof: After preparation of the manuscript we learnt of the related work of Rowley, Kevrekidis, Marsden and Lust [24] which builds on previous work by Rowley and Marsden [25]. In [25] the idea of splitting the solutions in the form (2.16) and adding a minimization condition like (2.26), appears in the context of Karhunen-Loève expansion for systems with symmetry. Equation (2.18) is then called the reconstruction equation. In [24] the authors generalize this approach to dynamical systems with self-similar symmetries, which, in addition to the equivariance used in this paper, allow rescalings of the time variable. Applications to traveling waves in one space dimension (Kuramoto-Shivashinsky, Burgers) are presented in [25],[24].

2. The general approach.

2.1. Equivariant evolution equations. In this section we set up the technique of decomposing the solutions of the evolution equation (1.1) in an abstract setting. Simultaneously, we treat two important examples (parabolic systems on the line and in the plane) in a formal way with the details of a proper functional analytic setting given in the subsequent sections. We assume that $(X, ||\cdot||)$ is a Banach space and Y is a dense subspace on which the operator F from (1.1) is defined, i.e.

$$F : \begin{array}{c} Y \subset X \to X \\ u \mapsto F(u) \end{array}, \qquad \overline{Y} = X. \tag{2.1}$$

Example 2.1. *Consider the parabolic system*

$$u_t = Au_{xx} + f(u, u_x) =: F(u), \quad -\infty < x < \infty, \tag{2.2}$$

where $u(x,t) \in \mathbb{R}^m$, A is a positive definite $m \times m$ matrix and $f : \mathbb{R}^{2m} \to \mathbb{R}^m$ is assumed to be sufficiently smooth. If $f(0) = 0$ and if f and its first derivative are globally bounded then (2.1) holds for the choice

$$Y = H^2(\mathbb{R}, \mathbb{R}^m), \quad X = L^2(\mathbb{R}, \mathbb{R}^m). \tag{2.3}$$

Clearly, this excludes solutions that do not decay at $\pm\infty$ and a more general setting will be discussed in sections 2.4 and 3. In this example and in what follows we use $H^k(\mathbb{R}, \mathbb{R}^m), k \geq 2$ to denote the standard Sobolev space of functions that have generalized derivatives in L^2 up to order $k \geq 2$.

As a second example we mention the semilinear equation

$$u_t = A\Delta u + f(u) =: F(u), \quad x \in \mathbb{R}^2 \tag{2.4}$$

where $u(x,t)$ and A are as above and $f : \mathbb{R}^m \to \mathbb{R}^m$ satisfies appropriate smoothness and boundedness assumptions (see section 4).

We further assume that a finite dimensional (not necessarily compact) Lie group $(G, \circ)$ is given that acts on X via a representation in $GL(X)$, that is we have a

homomorphism
(cf.[6, Ch.4.3.1])

$$a : \begin{array}{c} G \to GL(X) \\ \gamma \mapsto a(\gamma) \end{array} \tag{2.5}$$

satisfying

$$a(\mathbb{1}) = I, \quad a(\gamma_1 \circ \gamma_2) = a(\gamma_1)a(\gamma_2). \tag{2.6}$$

Here $\mathbb{1}$ and I denote the unit elements in G and $GL(X)$ respectively.

Our main assumption is that the mapping F from (2.1) is *equivariant under the action of* G in the following sense.

HYPOTHESIS 2.2. *For all* $\gamma \in G$

$$a(\gamma)(Y) \subseteq Y, \tag{2.7}$$
$$F(a(\gamma)u) = a(\gamma)F(u) \quad \forall u \in Y. \tag{2.8}$$

In the last equation we restrict the equivariance condition to the dense subspace Y. Equation (2.7) is included to ensure that $a(\gamma)$ maps the domain of F into itself. Note that (2.7) implies $a(\gamma)(Y) = Y$ since for every $\gamma \in G$

$$Y = a(\gamma)a(\gamma^{-1})(Y) \subseteq a(\gamma)(Y) \subseteq Y.$$

EXAMPLE 2.3. *Consider Example 2.1 with the additive group* $(G, \circ) = (\mathbb{R}, +)$ *and the action* $a(\gamma)$ *defined by the shift*

$$[a(\gamma)u](x) := u(x - \gamma), \quad x \in \mathbb{R}, \gamma \in G. \tag{2.9}$$

With the spaces from(2.3) equations (2.7) and (2.8) are satisfied .

In case (2.4) we take the two dimensional Euclidean group (see [6], [28], [29], [10])

$$G = SE(2) = S^1 \ltimes \mathbb{R}^2,$$

where the semi-direct product $S^1 \ltimes \mathbb{R}^2$ is defined topologically by the direct product

$$\gamma = (\theta, b) \in S^1 \times \mathbb{R}^2$$

and the group operation is given by

$$\gamma_1 \circ \gamma_2 = (\theta_1, b_1) \circ (\theta_2, b_2) = (\theta_1 + \theta_2, b_1 + \varrho_{\theta_1} b_2). \tag{2.10}$$

Here the unit element is $\mathbb{1} = (0, 0)$ and we write rotations in $\mathbb{R}^2$ as

$$\varrho_\theta = \begin{pmatrix} \cos(\theta) & -\sin(\theta) \\ \sin(\theta) & \cos(\theta) \end{pmatrix}. \tag{2.11}$$

The action on functions is given by (see [6],[29],[10])

$$[a(\gamma)u](x) := u(\varrho_{-\theta}(x - b)), \quad x \in \mathbb{R}^2. \tag{2.12}$$

One easily verifies the property (2.6) and the equivariance condition (2.8) with the help of the Euclidean equivariance of the Laplacian

$$\Delta_x [u(\varrho_\theta x)] = \Delta u(\varrho_\theta x), \quad \Delta_x [u(x - b)] = \Delta u(x - b).$$

2.2. Separating the group motion. A well known problem in the infinite dimensional setting is differentiability of the group action (see [28],[29], [10] for a detailed discussion). Neither can we expect the mapping a to be differentiable from G into $GL(X)$ nor can we assume that the mapping $\gamma \mapsto a(\gamma)u$ is differentiable for any fixed $u \in X$. Our assumption is

HYPOTHESIS 2.4. *For any $v \in X$ the mapping*

$$a(\cdot)v : \begin{array}{l} G \to X \\ \gamma \mapsto a(\gamma)v \end{array} \tag{2.13}$$

is continuous and for any $v \in Y$ it is continuously differentiable with derivative

$$a_\gamma(\gamma)v : \begin{array}{l} T_\gamma G \to X \\ \lambda \mapsto [a_\gamma(\gamma)v]\ \lambda \end{array} \tag{2.14}$$

We use $\mathcal{A}_\gamma = T_\gamma G$ to denote the tangent space of G at γ. Note that $\mathcal{A} := \mathcal{A}_{\mathbb{1}}$ is the Lie algebra associated with G which has the same dimension as G. A general principle of constructing spaces that satisfy Hypothesis 2.4 will be discussed in section 2.4.

For the example 2.3 continuity is satisfied for $v \in L^2(\mathbb{R}, \mathbb{R}^m)$ and continuous differentiability holds for functions $v \in H^1(\mathbb{R}, \mathbb{R}^m) \supset Y = H^2(\mathbb{R}, \mathbb{R}^m)$ with

$$[a_\gamma(\gamma)v]\,\lambda = -v_x(\cdot - \gamma)\lambda. \tag{2.15}$$

Consider a solution $u(t)$ of (1.1) and a function $\gamma \in C^1(\mathbb{R}, G), \gamma(0) = \mathbb{1}$ and define $v(t)$ via (see Figure 2.1)

$$u(t) = a(\gamma(t))v(t). \tag{2.16}$$

Then by differentiating formally and using the equivariance condition we obtain

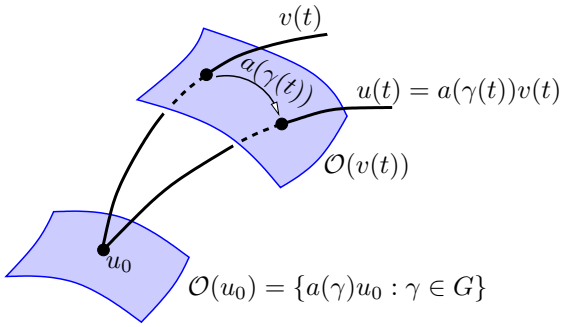

FIG. 2.1. *Splitting off the group dynamics by extension*

$$u_t = [a_\gamma(\gamma)v]\,\gamma_t + a(\gamma)v_t = F(u) = F(a(\gamma)v) = a(\gamma)F(v). \tag{2.17}$$

Applying $a(\gamma^{-1}) = a(\gamma)^{-1}$ to both sides we end up with the equation for the 'frozen solution' $v(t)$

$$v_t = F(v) - a(\gamma^{-1})a_\gamma(\gamma)v\gamma_t, \quad v(0) = u_0. \tag{2.18}$$

In order to make the equivalence of (1.1) and (2.18) rigorous we use a working definition for solutions which shares at least some properties of strong solutions for evolution

equations with C^0 semigroups (see [17],[28],[29],[10] for the standard solution concept in fractional order spaces when $F = A + f$ with a sectorial operator A).

DEFINITION 2.5. *A function $u \in C([0,T),X) \cap C^1((0,T),X)$ is called a solution of the initial value problem (1.1) on $[0,T)$ if $u(0) = u_0$, $u(t) \in Y$ for $0 < t < T$ and if the differential equation holds in the open interval $(0,T)$.*

With this notion we obtain the following Theorem.

THEOREM 2.6. *Suppose that the Hypotheses 2.2 and 2.4 hold and let $\gamma \in C^1([0,T),G)$ satisfy $\gamma(0) = \mathbb{1}$. Then u is a solution of (1.1) if and only if v, given by (2.16), is a solution of (2.18).*

Proof. We may write (2.16) equivalently as $v(t) = a(\gamma(t)^{-1})u(t)$ where $\gamma^{-1} \in C^1([0,T),G)$ and $\gamma^{-1}(0) = \mathbb{1}$. Therefore, it is sufficient to show that $u(t)$ inherits the smoothness from $v(t)$ and that the first equality in (2.17) holds. As in semigroup theory one concludes from Hypothesis 2.4 and the uniform boundedness principle that the operator norms $|a(\gamma)|$ are uniformly bounded when γ varies in a compact set. This implies continuity of the map $(\gamma,u) \mapsto a(\gamma)u$ on $G \times X$ and thus continuity of $u(t)$ for $t \in [0,T)$. Differentiability in $(0,T)$ and the desired formula follow from Hypothesis 2.4 by a careful look at the standard proof of chain and product rule:

$$\begin{aligned} u(t+h) - u(t) &= a(\gamma(t+h))(v(t+h) - v(t) - v_t(t)h) + a(\gamma(t))v_t(t)h + \\ &\quad (a(\gamma(t+h)) - a(\gamma(t)))v_t(t)h + (a(\gamma(t+h)) - a(\gamma(t)))v(t) \\ &= a(\gamma(t))v_t(t)h + [a_\gamma(\gamma(t))v(t)]\,\gamma_t(t)h + o(h). \end{aligned}$$

□

In (2.18) the path $\gamma(t)$ in the group is still arbitrary. We fix these degrees of freedom by so called 'phase conditions' the number of which equals the dimension of the group. We assume that we are given a map

$$\psi : \begin{array}{l} X \times G \to \mathcal{A}^* \\ (u,\gamma) \mapsto \psi(u,\gamma), \end{array} \tag{2.19}$$

that satisfies the consistency relation $\psi(u_0,\mathbb{1}) = 0$. In (2.19) we use $\mathcal{A}^*$ to denote the dual of the Lie algebra $\mathcal{A}$. Further introducing the variable $\lambda = \gamma_t$ we finally arrive at the following **PDAE** (Partial Differential Algebraic Equation) for the time-dependent variables $\gamma(t) \in G, \lambda(t) \in T_{\gamma(t)}G, v(t) \in Y$

$$v_t = F(v) - a(\gamma^{-1})a_\gamma(\gamma)v\lambda, \qquad v(0) = u_0 \tag{2.20}$$

$$\gamma_t = \lambda, \qquad \gamma(0) = \mathbb{1} \tag{2.21}$$

$$0 = \psi(v,\gamma). \tag{2.22}$$

In general (2.20) is a PDE, (2.21) an ODE system on a manifold and (2.22) is an algebraic constraint. In our example (2.2),(2.3) the PDAE reads

$$v_t = Av_{xx} + f(v,v_x) + v_x\lambda, \qquad v(0) = u_0 \tag{2.23}$$

$$\gamma_t = \lambda, \qquad \gamma(0) = 0 \tag{2.24}$$

$$0 = \psi(v,\gamma). \tag{2.25}$$

REMARK 2.7. *Decomposing the solution as in (2.16) is also the underlying idea in the center manifold reduction in [28],[29],[10] as well as in the slice theorem, see [6, Ch.6]. However, rather than using it to derive a reduced system which contains*

global terms from elimination, we set up an extended system that keeps most of the structure of the original problem. This will be better suited for numerical methods. We extend Definition 2.5 by saying that the tuple (v,γ,λ) is a solution of the PDAE on $[0,T)$ if $v \in C([0,T),X)\cap C^1((0,T),X)$ and $(\gamma,\lambda)\in C^1([0,T),TG)$ such that $v(t)\in Y$ for $0<t<T$ and such that the differential equation in (2.20) holds in $(0,T)$ and the equations in (2.21),(2.22) hold in $[0,T)$. Note that the tangent bundle TG consists of pairs (γ,λ) with $\lambda\in T_\gamma G$.

For the phase condition we use the following

HYPOTHESIS 2.8. *$\psi\in C^1(X\times G,\mathcal{A}^*), \psi(u_0,\mathbb{1})=0$ and the linear map*

$$\psi_\gamma(u_0,\mathbb{1})-\psi_v(u_0,\mathbb{1})a_\gamma(\mathbb{1})u_0 : \mathcal{A}\mapsto\mathcal{A}^*$$

is nonsingular.

The first part of the following theorem is an immediate consequence of Theorem 2.6.

THEOREM 2.9. *If (v,γ,λ) is a solution of (2.20)-(2.22) on $[0,T)$ then $u(t)=a(\gamma(t))v(t)$ solves (1.1). Conversely, assume that $u(t)$ solves (1.1) on some interval $[0,T)$ and that ψ satisfies Hypothesis 2.8. Then there exists an interval $[0,\tau)\subset[0,T)$ and a function $\gamma\in C^1([0,\tau),G)$ such that $(v=a(\gamma^{-1})u,\gamma,\lambda=\gamma_t)$ is a solution of (2.20)-(2.22) on $[0,\tau)$.*

Proof. For the second part apply the implicit function theorem to the equation

$$\varphi(\gamma,t):=\psi(a(\gamma^{-1})u(t),\gamma)=0.$$

Note that $\varphi(\mathbb{1},0)=0$ and that $\varphi_\gamma(\mathbb{1},0)=\psi_\gamma(u_0,\mathbb{1})-\psi_v(u_0,\mathbb{1})a_\gamma(\mathbb{1})u_0$ is invertible by Hypothesis 2.8. ∎

2.3. Phase conditions. Let us assume that we have an inner product $\langle\cdot,\cdot\rangle$ on X that is continuous with respect to the given norm $||\cdot||$, i.e. $|u|=\sqrt{\langle u,u\rangle}\le C||u||$. For equation (2.3) in Example 2.1, the two norms are identical and X is a Hilbert space, but we do not assume this is general. In later applications we will use weighted and locally uniform norms for which the two norms differ.

One way to set up a phase condition is to minimize the distance of the frozen solution v from the group orbit of the starting value

$$\mathcal{O}(u_0)=\{a(\gamma)u_0 : \gamma\in G\}$$

i.e. minimize $e_1(\gamma)=|a(\gamma)u_0-v|^2$. If we require u_0 to be the point on the orbit that is closest to v we obtain from Hypothesis 2.4 the necessary condition

$$\psi_1(v,\gamma)\mu:=\langle a_\gamma(\mathbb{1})u_0\mu,u_0-v\rangle=0\quad\forall\mu\in\mathcal{A}. \tag{2.26}$$

Similarly, we may require that v is the point of minimal distance from u_0 on $\mathcal{O}(v)$, i.e. we minimize $e_2(\gamma)=|u_0-a(\gamma)v|^2$. This leads to (see Figure 2.2 for an illustration)

$$\psi_2(v,\gamma)\mu:=\langle a_\gamma(\mathbb{1})v\mu,u_0-v\rangle=0\quad\forall\mu\in\mathcal{A}. \tag{2.27}$$

PROPOSITION 2.10. *If the isotropy subgroup (or stabilizer) of u_0, given by*

$$Stab(u_0)=\{\gamma\in G : a(\gamma)u_0=u_0\}$$

is trivial, then both phase conditions (2.26) and (2.27) satisfy Hypothesis 2.8.

FIG. 2.2. *Minimizing the distance of v to $\mathcal{O}(u_0)$ (left) or of u_0 to $\mathcal{O}(v)$ (right)*

Proof. It is well known (see [6, Th.4.3.4]) that

$$\dim(\mathcal{O}(u_0)) = \dim(T_{u_0}\mathcal{O}(u_0)) = \dim(G) - \dim(\mathrm{Stab}(u_0)).$$

Let d be the dimension of G. Then we can choose elements $g_i \in \mathcal{A}, i = 1, \dots, d$ such that $S_i = [a_\gamma(\mathbb{1})u_0]g_i$ form a basis of $T_{u_0}\mathcal{O}(u_0)$. By a direct calculation we have for $\lambda, \mu \in \mathcal{A}$

$$-[\psi_{1,v}(u_0, \mathbb{1})a_\gamma(u_0)\lambda]\mu = \langle a_\gamma(\mathbb{1})u_0\mu, a_\gamma(\mathbb{1})u_0\lambda\rangle. \tag{2.28}$$

Therefore, $\psi_{1,v}(u_0, \mathbb{1})a_\gamma(u_0)\lambda : \mathcal{A} \mapsto \mathcal{A}^*$ is nonsingular iff the $d \times d$-matrix with entries $\langle S_i, S_j\rangle$ is nonsingular. Clearly this holds if and only if the S_i are linearly independent. For the second phase condition (2.27) note that we obtain the same expression (2.28). ∎

REMARK 2.11. *If the inner product is G-invariant then $e_1(\gamma) = e_2(\gamma^{-1})$ and the two minimization problems are equivalent. Moreover, the two necessary conditions (2.26) and (2.27) are identical, since we have $\langle a_\gamma(\mathbb{1})v, v\rangle = 0$ for $v \in Y$. The last equation follows by differentiating $\langle a(\gamma)v, a(\gamma)v\rangle = \langle v, v\rangle$ at $\gamma = \mathbb{1}$.*

In equivariant bifurcation theory interesting phenomena arise when the isotropy group of some relative equilibrium is nontrivial, see [10],[6]. For an initial value problem with some 'generic' u_0, however, it seems reasonable to assume a trivial isotropy subgroup.

The remark applies to the parabolic system (2.23)-(2.25) with spaces (2.3). In this case the phase conditions (2.26) and (2.27) yield the integral constraint

$$0 = \psi(v) = \int_{-\infty}^{\infty} u_{0,x}^T(u_0 - v)\, dx = -\int_{-\infty}^{\infty} u_{0,x}^T v\, dx \tag{2.29}$$

Hypothesis 2.8 requires the map $\lambda \to \lambda \int_{-\infty}^{\infty} u_{0,x}^T u_{0,x}\, dx$ to be nonsingular which is satisfied if u_0 is nonconstant.

The phase conditions developed so far depend on the initial value u_0 and seem to be useful only for short times, see Theorem 2.9. During numerical computations one could update the phase condition by using $v(t_1), v(t_2), \dots$ at later times instead of u_0.

A condition that is applicable in a more global sense is to minimize the temporal change of v, i.e.

$$|v_t|^2 = |F(v) - a(\gamma^{-1})a_\gamma(\gamma)v\lambda|^2. \tag{2.30}$$

This is a d-dimensional least squares problem in $\lambda \in \mathcal{A}_\gamma$. We introduce the operators

$$S(v, \gamma) = a(\gamma^{-1})a_\gamma(\gamma)v : \mathcal{A}_\gamma \mapsto X \tag{2.31}$$

and $S^*(v,\gamma) : X \mapsto \mathcal{A}_\gamma^*$ by

$$[S^*(v,\gamma)u]\lambda = \langle S(v,\gamma)\lambda, u\rangle \quad \text{for } \lambda \in \mathcal{A}_\gamma. \tag{2.32}$$

If the stabilizer of $a(\gamma)v$ is trivial then $S(v,\gamma)$ is one to one and $S^*S(v,\gamma) \in L(\mathcal{A}_\gamma, \mathcal{A}_\gamma^*)$ is nonsingular. Therefore, (2.30) has a unique minimizer given by the solution of the linear $d \times d$ system

$$\psi_{\min}(v,\gamma,\lambda) := (S^*S)(v,\gamma)\lambda - S^*(v,\gamma)F(v) = 0. \tag{2.33}$$

Note that in contrast to (2.25) this phase condition depends also on the derivative $\gamma_t = \lambda$ so that Theorem 2.9 does not apply. Nevertheless, a given solution $u(t), t \in [0,T)$ of (1.1) may be written as $u(t) = a(\gamma(t))v(t)$ with v satisfying (2.20) and (γ,λ) satisfying (2.33) if we determine $\gamma(t)$ from the following initial value problem on G

$$\gamma_t(t) = [(S^*S)^{-1}S^*](a(\gamma^{-1})u(t),\gamma)\; a(\gamma^{-1})F(u(t)), \quad \gamma(0) = \mathbb{1}. \tag{2.34}$$

In order to ensure a unique solution of this problem we need more regularity for $F(u(t)), t \in [0,T)$ than in Theorem 2.9, such that the right hand side of (2.34) is continuous in (γ,t) and locally Lipschitz in γ.

More details on the implementation of the phase condition (2.33) will be given in the next sections. The condition turns out to be particularly useful near relative equilibria of (1.1) where we expect v_t to tend to zero.

A final alternative is to require that at any time instance, v_t is orthogonal to the group orbit $\mathcal{O}(u) = \mathcal{O}(a(\gamma)v)$ at v, (see Figure 2.3).

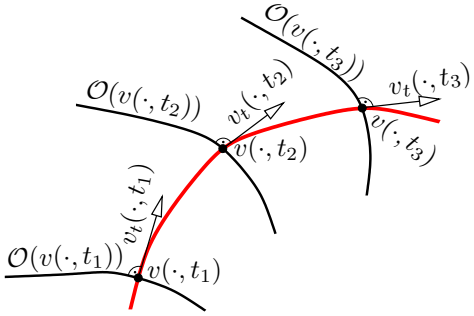

FIG. 2.3. *Orthogonality of time and group orbit at successive times*

This leads to the condition

$$0 = \langle S(v,\mathbb{1})\mu, v_t\rangle \quad \forall \mu \in \mathcal{A}_\gamma.$$

Using the differential equation (2.20) we rewrite the phase condition as

$$\psi_{\text{orth}}(v,\gamma,\lambda) = S^*(v,\mathbb{1})S(v,\gamma)\lambda - S^*(v,\mathbb{1})F(v) = 0. \tag{2.35}$$

Note that this condition is identical with (2.33) if $a(\gamma^{-1})a_\gamma v$ does not depend on γ.

For example, it is true for the parabolic system (2.23)-(2.25) (and for most of the examples in sections 3 and 4). Conditions (2.33) and (2.35) both lead to the explicit formula

$$\langle v_x, v_x\rangle_{L^2}\lambda = \langle v_x, Av_{xx} + f(v,v_x)\rangle_{L^2} = \langle v_x, f(v,v_x)\rangle_{L^2}, \tag{2.36}$$

which works whenever the function v is nonconstant. Note that the last equality follows from $v \in H^2(\mathbb{R},\mathbb{R}^m)$ if $A = A^T$.

2.4. Construction of spaces. In [29, Theorem 4.5] the authors set up a general principle for constructing spaces that satisfy the differentiability condition in Hypothesis 2.4. In the following proposition we slightly extend their result by constructing a sequence of nested spaces on which the group acts with increasing smoothness. We use the exponential map $\exp : \mathcal{A} \mapsto G$, cf. [6, Ch. 4.2].

PROPOSITION 2.12. *Let $(X_0, ||\cdot||_0)$ be a Banach space and let $a : G \mapsto GL(X_0)$ be a homomorphism. Then*

$$X_1 = \{u \in X_0 : ||u||_1 := \sup_{\gamma\in G} ||a(\gamma)u||_0 < \infty\}$$

is a Banach space with respect to the norm $||\cdot||_1$ and the operators $a(\gamma)_{|X_1}$ are isometries in $GL(X_1)$. Further, the space

$$X_2 = \{u \in X_1 : \gamma \mapsto a(\gamma)u \text{ is continuous in } G\}$$

is a closed subspace of $(X_1, ||\cdot||_1)$ such that $a(\gamma)_{|X_2} \in GL(X_2)$ acts strongly continuously. Finally,

$$X_3 = \{u \in X_2 : \gamma \mapsto a(\gamma)u \text{ is continuously differentiable in } G\}$$

is a dense subspace of X_2 and can be written as

$$X_3 = \bigcap_{\lambda\in\mathcal{A}} D(\lambda), \tag{2.37}$$

where $D(\lambda)$ is the domain of the infinitesimal generator of the C^0-semigroup $a(\exp(\lambda t))$, $t \geq 0$.

Proof. If $u_n \in X_1$ is a Cauchy sequence with respect to $||\cdot||_1$ then $a(\gamma)u_n$ is a Cauchy sequence in X_0 for each $\gamma \in G$ and hence converges to some $v(\gamma) \in X_0$. By continuity of $a(\gamma)$ we have $v(\gamma) = a(\gamma)v(\mathbb{1})$ and using the Cauchy property again we obtain $||u_n - u||_1 \to 0$ for $u = v(\mathbb{1})$ as well as $u \in X_1$. The isometric property of $a(\gamma)_{|X_1}$ is obvious and the closedness of X_2 with respect to $||\cdot||_1$ is an easy exercise. The main result in [29, Theorem4.5] states that $\bigcap_{\lambda\in\mathcal{A}} D(\lambda)$ is contained in X_3 and is a dense subspace of X_2. But the opposite inclusion $X_3 \subset \bigcap_{\lambda\in\mathcal{A}} D(\lambda)$ follows from the chain rule applied to $a(\exp(\lambda t))u, u \in X_3$ and this finishes the proof. □

REMARK 2.13. *Under the assumptions of the proposition we can satisfy Hypothesis 2.4 by taking $X = X_2$ and $Y = X_3$. However, in the applications the right hand side of (1.1) may contain differential operators that require an even smaller (but still dense) domain Y.*

EXAMPLE 2.14. *For $\gamma \in G = \mathbb{R}^N$ consider the shift (see (2.9))*

$$[a(\gamma)u](x) = u(x - \gamma), \quad x \in \mathbb{R}^N.$$

If we take $X_0 = C_b^0(\mathbb{R}^N, \mathbb{R}^m)$ (continuous bounded functions) with $||\cdot||_0$ as the sup-norm in Proposition 2.12 then we obtain $X_1 = X_0, ||\cdot||_1 = ||\cdot||_0$ and the spaces of uniformly contiuous functions $X_2 = C^0_{unif}(\mathbb{R}^N, \mathbb{R}^m), X_3 = C^1_{unif}(\mathbb{R}^N, \mathbb{R}^m)$.

Another choice are locally uniform spaces as proposed in [20], [19]. Take a positive and integrable weight function $\eta \in C^1(\mathbb{R}^N, (0, \infty)) \cap L^1(\mathbb{R}^N)$ that satisfies $|\nabla\eta(x)| \leq C\eta(x), \forall x \in \mathbb{R}^N$. For $p \geq 1$ consider the weighted L^p space

$$X_0 = L^p_\eta(\mathbb{R}^N) = \{u \in L_{loc}(\mathbb{R}^N, \mathbb{R}^m) : ||u||_{L^p_\eta} < \infty\}, \tag{2.38}$$

$$||u||_{L^p_\eta} = \left(\int_{\mathbb{R}^N} \eta(x)|u(x)|^p dx\right)^{\frac{1}{p}}. \tag{2.39}$$

From the estimate $\eta(x+\gamma) \le e^{C|\gamma|}\eta(x)$ *one finds that* $a(\gamma) : X_0 \mapsto X_0$ *is a bounded operator with bound* $e^{\frac{C|\gamma|}{p}}$. *The construction in Proposition 2.12 then yields the locally uniform spaces (using the notation from [20],[19])*

$$X_0 \supset X_1 = \tilde{L}^p_{ul}(\mathbb{R}^N) \supset X_2 = L^p_{ul}(\mathbb{R}^N). \tag{2.40}$$

Here the norm $||u||_{L^p_{ul}} = \sup_{\gamma\in\mathbb{R}^N} ||u(\cdot-\gamma)||_{L^p_\eta}$ *in* X_1 *is stronger than* $||\cdot||_0$ *and all inclusions are strict. Finally, the intersection of the domains of the infinitesimal generators* $\frac{\partial}{\partial x_j}, j = 1,\dots,N$ *leads to the weighted Sobolev space*

$$X_3 = W^{1,p}_{ul}(\mathbb{R}^N) = \{u \in L^p_{ul}(\mathbb{R}^N) : \frac{\partial u}{\partial x_j} \in L^p_{ul}(\mathbb{R}^N), j = 1,\dots,N\}. \tag{2.41}$$

3. Waves in one space dimension.

3.1. Relative equilibria. Following [10],[6] we define relative equilibria as solutions that stay in the group orbit of the initial value (see also [10] and [28] for the further notions of a relative periodic orbit and meandering solutions)

DEFINITION 3.1. *A solution* $u(t), t \in [0,T)$ *of equation (1.1) is called a relative equilibrium if there exist* $v \in Y, \gamma \in C^1([0,T),G)$ *such that* $\gamma(0) = \mathbb{1}$ *and*

$$u(t) = a(\gamma(t))v, \quad 0 \le t < T. \tag{3.1}$$

In view of (2.20),(2.21) this implies the following equations

$$0 = F(v) - S(v,\gamma(t))\lambda(t), \text{ where } \quad S(v,\gamma)\lambda = a(\gamma^{-1})a_\gamma(\gamma)v\lambda \tag{3.2}$$

$$\gamma_t(t) = \lambda(t), \quad \gamma(0) = \mathbb{1}. \tag{3.3}$$

In the applications we will frequently have relative equilibria for which the operator $S(\cdot,\gamma(t))\lambda(t) : Y \mapsto X$ is independent of t.

For example, a traveling wave

$$[u(t)](x) = v(x-\lambda t), \quad \gamma(t) = \lambda t \tag{3.4}$$

is an equilibrium of the system (2.23) with constant λ and a relative equilibrium of (2.2) (take any of the spaces from Example 2.14). Conversely, if $u(t) = a(\gamma(t))v$ is a relative equilibrium of (2.2), then with $\lambda = \gamma_t$ we have

$$0 = Av_{xx} + f(v,v_x) + v_x\lambda(t).$$

Taking the inner product with v_x and assuming that v is nonconstant we conclude that $\lambda(t)$ is in fact time independent. Hence, traveling waves are the only nontrivial relative equilibria of (2.2).

As a second example consider the complex valued system

$$u_t = Au_{xx} + f(u,u_x), \quad x \in \mathbb{R}, \quad u(x,t) \in \mathbb{C}^m, \tag{3.5}$$

where $f : \mathbb{C}^{2m} \mapsto \mathbb{C}^m$ is assumed to be equivariant with respect to phase factors

$$f(e^{i\theta}u, e^{i\theta}v) = e^{i\theta}f(u,v), \ \theta \in S^1 = \mathbb{R}/2\pi\mathbb{Z}. \tag{3.6}$$

Well known special cases are equations of *Ginzburg-Landau* type

$$f(u,v) = au + bu|u|^2 + cu|u|^4, \ u \in \mathbb{C}, \quad a,b,c \in \mathbb{C}. \tag{3.7}$$

In this case the Lie group is $G = S^1 \times \mathbb{R}$ with

$$(\theta_1, \tau_1) \circ (\theta_2, \tau_2) = (\theta_1 + \theta_2, \tau_1 + \tau_2) \tag{3.8}$$

and the action is given by

$$[a(\theta, \tau)v](x) = e^{-i\theta} v(x - \tau). \tag{3.9}$$

The system (2.20),(2.21) now reads

$$v_t = Av_{xx} + f(v, v_x) + iv\lambda_1 + v_x\lambda_2, \qquad v(0) = u_0, \tag{3.10}$$

$$\theta_t = \lambda_1,\ \tau_t = \lambda_2 \qquad \theta(0) = 0, \tau(0) = 0. \tag{3.11}$$

The phase condition (2.26) has the form

$$\psi_1(v, \theta, \tau) = (\langle iu_0, v - u_0\rangle, \langle u_{0,x}, v - u_0\rangle) = (0, 0), \tag{3.12}$$

where $\langle \cdot, \cdot \rangle$ is the inner product in the real system of doubled dimension, i.e.

$$\langle u + iv, w + iz\rangle_{L_2} = \int_{\mathbb{R}} u^T w + v^T z \; dx. \tag{3.13}$$

Hypothesis 2.8 is satisfied if the functions iu_0 and u_{0x} are linearly independent over $\mathbb{R}$. Relative equilibria of (3.5) are rotating waves

$$u(x, t) = e^{-i\lambda_1 t} v(x - \lambda_2 t), \quad x \in \mathbb{R},\ t \in \mathbb{R}, \tag{3.14}$$

where v is in one of the spaces $H^2(\mathbb{R}, \mathbb{C}^m), C^2_{\text{unif}}(\mathbb{R}, \mathbb{C}^m)$ or $H^2_{\text{ul}}(\mathbb{R}, \mathbb{C}^m) = W^{2,2}_{\text{ul}}(\mathbb{R}, \mathbb{C}^m)$, cf. Example 2.14. Similar to the previous example we obtain that these are the only relative equilibria for which iv and v_x are linearly independent.

3.2. Numerical computations. For the discretization in time and space we consider a system (2.2) that is equivariant under a Lie group of dimension d and that - with a proper choice of coordinates in G and TG - leads to a PDAE (2.20), (2.21) of the form

$$v_t = F(v) - S(v)\lambda, \quad S(v)\lambda = \sum_{j=1}^{d} S_j(v)\lambda_j, \qquad v(0) = u_0, \tag{3.15}$$

$$\gamma_t = \lambda, \qquad \gamma(0) = 0. \tag{3.16}$$

Here F is given by (2.2) and the S_j are linear differential operators of order ≤ 1 with bounded continous coefficients

$$S_j(v) = B_j(x)v_x + C_j(x)v, \quad B_j, C_j \in C^0_b(\mathbb{R}, \mathbb{R}^{m,m}).$$

For the phase condition we use the orthogonality constraint (2.35), which in this case is the same as (2.33)

$$\psi_{\text{orth}}(v, \lambda) = (\langle S_\nu(v), \sum_{j=1}^{d} S_j(v)\lambda_j - F(v)\rangle)_{1 \le \nu \le d} = 0, \tag{3.17}$$

where $\langle \cdot, \cdot \rangle$ is the inner product in either L^2 or in L^2_η.

We choose a step size Δt in time and an equidistant spatial grid

$$J = \{x_j = j\Delta x : 0 \le j \le M\}, \quad \Delta x = \frac{x_+ - x_-}{M},$$

where $[x_-, x_+]$ is some large interval. At time $t_n = n\Delta t$ we compute the approximations $\gamma^n, \lambda^n \in \mathbb{R}^d$ and $v^n : J \mapsto \mathbb{R}^m$ by a half-explicit Euler method, i.e. a method that is explicit in the state variable v^n but implicit in the algebraic variable λ^n (see [15],[16] for such methods)

$$\frac{1}{\Delta t}(v^{n+1} - v^n) = F_{\Delta x}(v^n) - S_{\Delta x}(v^n)\lambda^{n+1}, \tag{3.18}$$

$$\frac{1}{\Delta t}(\gamma^{n+1} - \gamma^n) = \frac{1}{2}(\lambda^{n+1} + \lambda^n), \tag{3.19}$$

$$0 = (\langle S_{\nu,\Delta x}(v^n), \sum_{j=1}^{d} S_{j,\Delta x}(v^n)\lambda_j^{n+1} - F_{\Delta x}(v^n)\rangle)_{1\le\nu\le d}. \tag{3.20}$$

Here $F_{\Delta x}$ and $S_{\Delta x}$ are standard finite difference approximations

$$F_{\Delta x}(v) = D_+D_-v + f(v, D_0v), \quad S_{j,\Delta x}(v) = B_jD_0v + C_jv,$$

where $D_\pm$ denote forward/backward and $D_0 = \frac{1}{2}(D_+ + D_-)$ centered difference quotients. In any time step one first solves the linear $d \times d$ system (3.20) for λ^{n+1} and then determines v^{n+1}, γ^{n+1} from (3.18),(3.19). Standard stability restrictions such as $\Delta t \le \frac{1}{2}(\Delta x)^2$ are taken into account.

Equation (3.18) has to be completed by boundary conditions. We choose Neumann and projection boundary conditions.

For traveling waves (more generally relative equilibria) projection boundary conditions are in common use as asymptotic boundary conditions at $x_\pm$ in order to have higher order approximations of wave form and speed (see [4],[26]). We adapt them to the time-dependent case as follows. Assume that the limits $\lim_{x\to\pm\infty} C_j(x) = C_{j,\pm}$ exist and the solution satisfies

$$\lim_{x\to\pm\infty} v(x,t) = w_\pm, \ \lim_{x\to\pm\infty} v_x(x,t) = 0, \ f(w_\pm, 0) - \sum_{j=1}^{d} C_{j,\pm}w_\pm = 0. \tag{3.21}$$

The idea behind projection b.c. is to control the growing resp. decaying spatial modes obtained by linearizing at $\pm\infty$. We write the conditions in the form

$$V_\pm(v(x_\pm) - w_\pm) + W_\pm v_x(x_\pm) = 0, \tag{3.22}$$

where $V_\pm, W_\pm \in \mathbb{R}^{m,m}$. These matrices can be obtained by setting $W_\pm = Z_\pm A, V_\pm = -\Lambda_\pm^{-1}Z_\pm C_\pm$ where $\Lambda_+, \Lambda_- \in \mathbb{R}^{m,m}$ have only eigenvalues with real part positive resp. negative and where $Z_\pm \in \mathbb{R}^{m,m}$ form a corresponding invariant subspace of the 'left quadratic eigenvalue problem'

$$\Lambda_\pm^2 Z_\pm A + \Lambda_\pm Z_\pm B_\pm + Z_\pm C_\pm = 0, \tag{3.23}$$

$$B_\pm = D_2 f(w_\pm, 0) + \sum_{j=1}^{d} B_{j,\pm}\lambda_j, \quad C_\pm = D_1 f(w_\pm, 0) + \sum_{j=1}^{d} C_{j,\pm}\lambda_j. \tag{3.24}$$

In the n-th time step one has to set $\lambda = \lambda^n$ in (3.24) and so the projection boundary conditions (3.22) depend on time.

3.3. Numerical Examples. In the following we test our method on several well known examples of parabolic systems that show traveling or rotating waves.

3.3.1. Nagumo wave. The Nagumo equation [21], [22]

$$u_t = u_{xx} + u(1-u)(u-\alpha),\ u(x,0) = u_0(x), \quad \alpha \in (0, \frac{1}{2}) \tag{3.25}$$

has an explicit traveling wave solution $u(x,t) = \bar{v}(x-ct)$ given by

$$\bar{v}(x) = \frac{1}{1+\exp(-\frac{x}{\sqrt{2}})}, \quad c = -\sqrt{2}\ (\tfrac{1}{2} - \alpha).$$

For the numerical computations we use parameters $\alpha = \frac{1}{4}$, $J = [-30, 30]$, $\Delta x = 0.1$, $\Delta t < \frac{1}{2}\Delta x^2$ and Neumann boundary conditions.

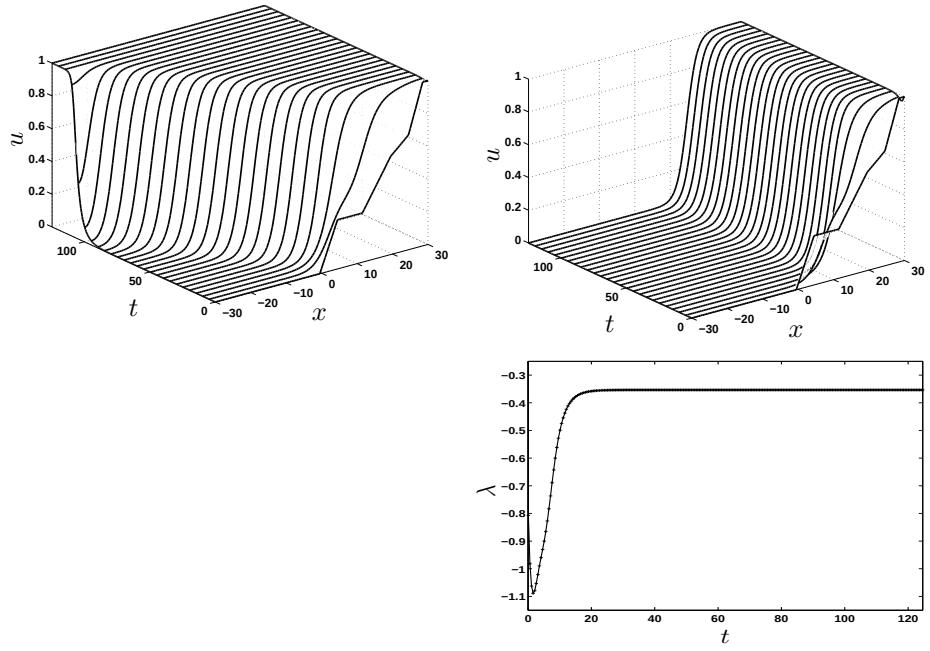

FIG. 3.1. *Traveling vs. frozen Nagumo wave and evolution of velocity* $\lambda(t)$.

In Figure 3.1 we compare the time evolution of a piecewise linear initial profile for the unmodified equation with its frozen counterpart computed from (3.18)-(3.20). The frozen profile stabilizes after short time and the parameter $\lambda(t)$ converges to a fixed value $\lambda_\infty = -0.353555$, which is in good agreement with the velocity of the exact solution on $\mathbb{R}$. In contrast to this, the solution of the original equation becomes constant when the wave reaches the left boundary. The reason is, of course, that the constants $0, 1$ and α are the only solutions of the stationary boundary value problem on the finite interval. While the evolution problems (3.25) and (3.15),(3.16) are equivalent on the whole real line (compare Theorem 2.6) they become different when truncated to a finite interval. In Figure 3.2 we compare two frozen equations with different

boundary conditions (Neumann and asymptotic) on a rather short interval $J = [-4, 4]$. While asymptotic boundary conditions still admit a stationary profile close to the original wave, Neumann b.c. allow only constant stationary profiles as solutions of the corresponding frozen equation in the limit $t \to \infty$.

On the larger interval $J = [-8, 8]$ Neumann b.c. are acceptable again, see Figure 3.3. The solutions for both boundary conditions differ by an amount of the order 10^{-3} which cannot be seen in the scale of Figure 3.3(a). Therefore, we show in Figure 3.3(b) the difference in λ as a function of time. Summarizing, the pictures demonstrate that the advantages of projection b.c. for the computation of stationary profiles carry over to the time-dependent case.

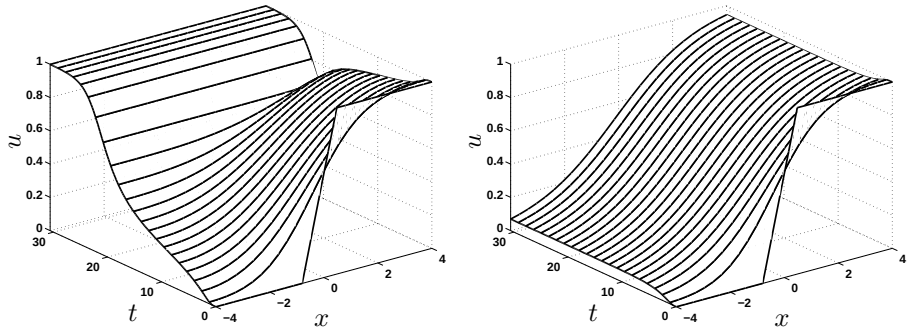

(a) Neumann b.c. (b) Asymptotic b.c.

FIG. 3.2. *Frozen Nagumo wave on* $J = [-4, 4]$

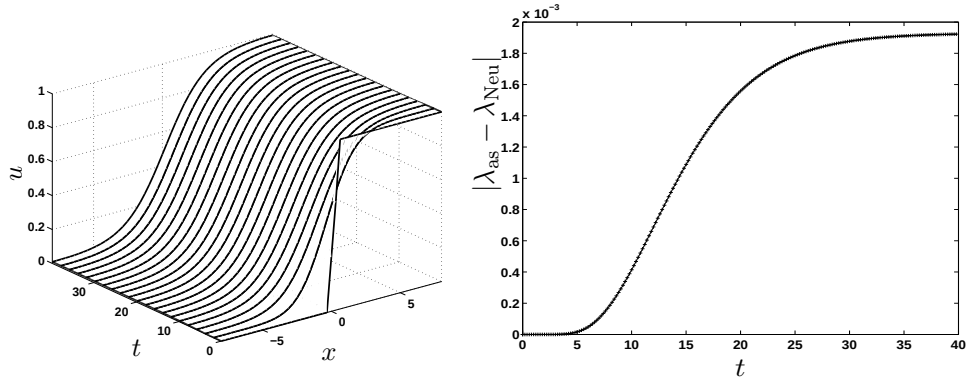

(a) Wave profile (b) Difference to asymptotic b.c. in λ

FIG. 3.3. *Frozen Nagumo wave on* $J = [-8, 8]$*, Neumann boundary conditions*

3.3.2. FitzHugh-Nagumo wave. A well-known two-component system with traveling wave solutions is given by the FitzHugh-Nagumo equations [21], [22]

$$V_t = \Delta V + V - \frac{1}{3}V^3 - R,$$
$$R_t = \phi(V + a - bR)$$

with parameters $a = 0.7,\ b = 0.8,\ \phi = 0.08$. As in the Nagumo case, the equation is equivariant with respect to translation. The numerical parameters are $J = [0, 130],\ \Delta x = 0.5$ and $\Delta t = 0.01$ with Neumann boundary conditions.

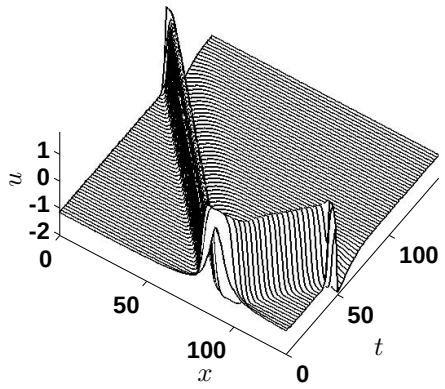

FIG. 3.4. *FHN, traveling wave*

In Figure 3.4 the time evolution of the V-component of a given initial profile (R has been set initially to the stationary value $\bar{R} = -0.62426$) is shown. The initial hump splits into two traveling components and after some time only the left moving pulse exists and leaves the computational window. Figure 3.5 shows the solution of the frozen equation starting from the same profile. As before the initial profile splits into a left and a right traveling pulse. When the right moving solution has left J, the remaining pulse stabilizes and takes the shape of the well known stable pulse (see [21]). The parameter $\lambda(t)$ converges after a transition phase to $\lambda_\infty = -0.816848$. As we see in this example, our method can only freeze one wave at a time. Which one is selected, depends on the type of phase condition used.

In Figure 3.5(a) the adaptive phase condition (3.17) is used and the left moving pulse is frozen. If we use the fixed phase condition (2.26) as shown in Figure 3.5(b) the right moving pulse stabilizes at the position of the initial hump.

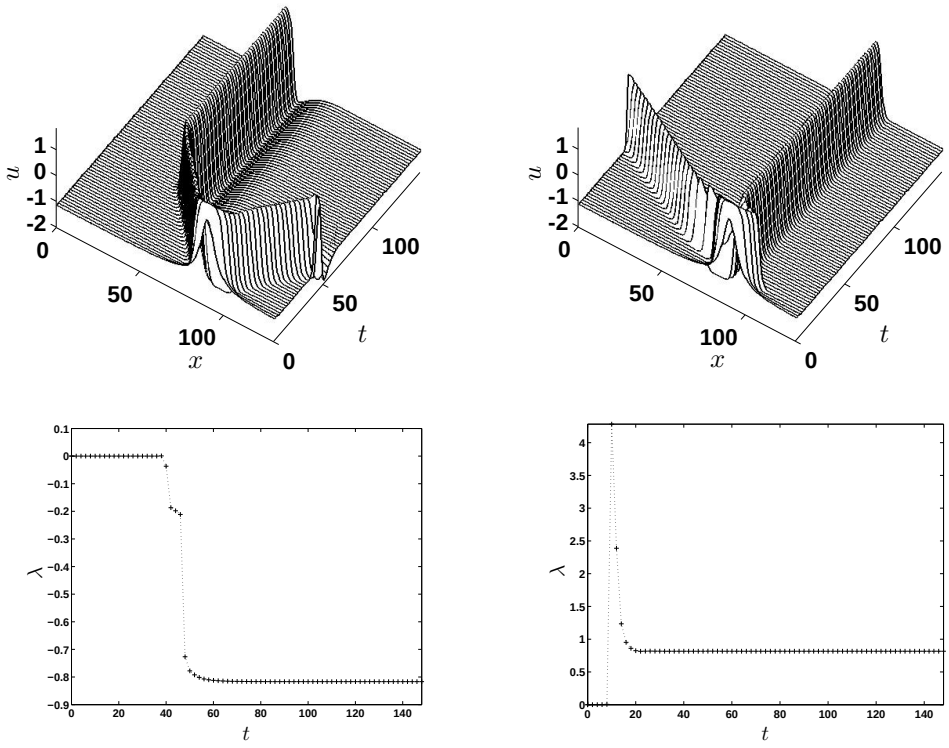

(a) Phase condition (3.17)

(b) Phase condition (3.12)

FIG. 3.5. *FHN, frozen wave*

3.3.3. The complex Ginzburg-Landau equation. We consider a special normalization of the complex Ginzburg Landau equation discussed in [19]

$$u_t = (1+i\alpha)(u_{xx} - (1+i\omega)^2 u + (1+i\omega)(2+i\omega)|u|^2 u), \quad u = u_1 + iu_2. \tag{3.26}$$

Here α and ω are real parameters. As described in section 3.1 this equation is equivariant under the action of the symmetry group $G = S^1 \times \mathbb{R}$.

One finds rotating wave solutions of the form $u(x,t) = e^{i\phi t}u_0$ with a profile u_0 which is constant in x. Inserting this ansatz into (3.26) one obtains for the absolute value of the solution u_0 and for the angular velocity ϕ the formulas

$$|u_0|^2 = \frac{\omega^2 + 2\alpha\omega - 1}{\omega^2 + 3\alpha\omega - 2}, \quad \phi = (\alpha(2-\omega^2) + 3\omega)|u_0|^2 + \alpha(\omega^2 - 1) - 2\omega.$$

For the numerical computations we choose parameters $\omega = -2,\ \alpha = \frac{1}{4},\ J = [-30, 30]$, $\Delta x = 0.5,\ \Delta t = 0.001$ and Neumann boundary conditions. We start from an initial profile which consists of small Gaussian pulses for the components u_1 and u_2.

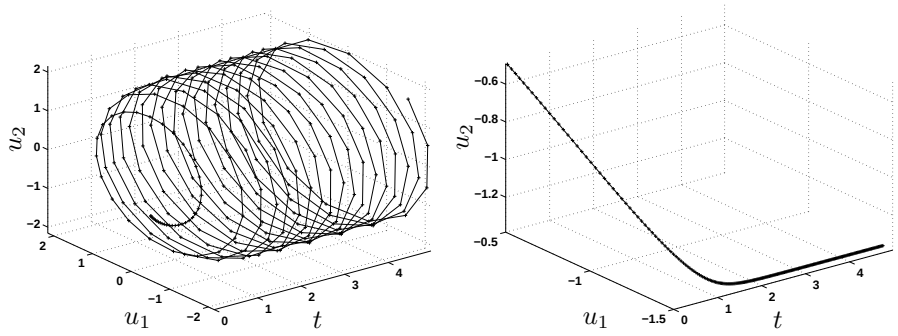

(a) Rotating solution (b) Frozen solution

FIG. 3.6. *Complex Ginzburg-Landau system, rotating vs. frozen solution.*

In Figure 3.6 the time evolution of the point $u(0,t)$ of the solution for the rotating and the frozen system are compared. The frozen solution stabilizes after some time at a fixed value whereas the solution of the original system continues rotating.

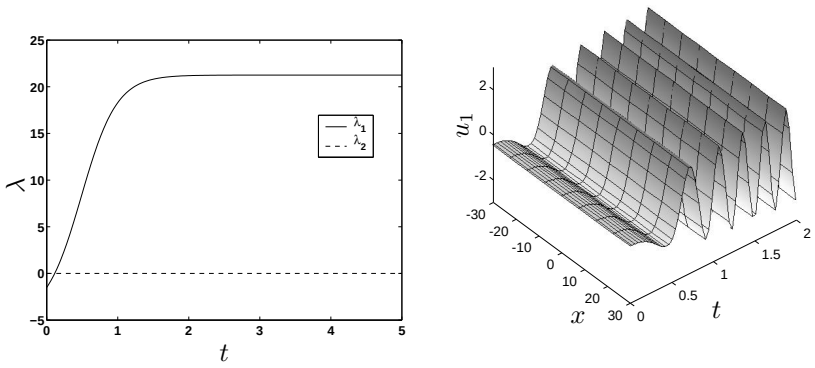

(a) Evolution of $\lambda_1 = \dot{\theta},\ \lambda_2 = \dot{\tau}$ (b) Evolution of the initial profile

FIG. 3.7. *Complex Ginzburg-Landau equation.*

As shown in Figure 3.7(a) the parameter $\lambda_1(t) = \dot{\theta}(t)$ converges to the exact angular velocity $\phi = 21.25$ and the translational speed $\lambda_2(t) = \dot{\tau}(t)$ stays at zero, as expected. The evolution of the whole profile of the u_1 component of the rotating solution is depicted in Figure 3.7(b).

Figure 3.8 demonstrates the advantage of the half-explicit scheme for the frozen system over the explicit scheme for the original system. We compare the discretized analog of the normalized L^2 norm of the solution $\|u(\cdot,t)\|_n = \sqrt{\frac{1}{|J|}\int_J \|u(x,t)\|^2\ dx}$ for the frozen and the rotating system. Since the parameter λ is computed implicitly from the phase condition (3.20) the norm $\|u(\cdot,t)\|_n$ converges for the frozen system to the exact value of 2 whereas in the rotating system the norm is overestimated due to the use of the explicit Euler method.

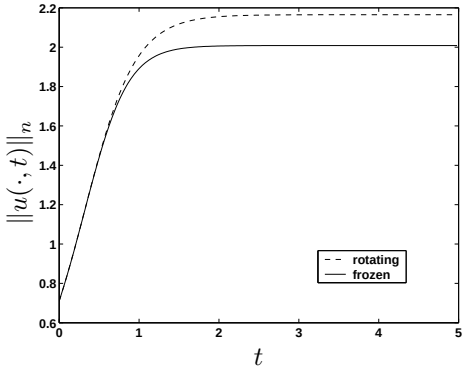

FIG. 3.8. $\|u(\cdot,t)\|_n$, *rotating vs. frozen system.*

4. Spiral waves in two dimensions.

4.1. The PDAE for Euclidean symmetry. Consider the semilinear parabolic system (2.4), i.e.

$$u_t = A\Delta u + f(u), \quad x \in \mathbb{R}^2, t \geq 0, \quad u(\cdot, 0) = u_0, \tag{4.1}$$

where $A \in \mathbb{R}^{m,m}$ is positive definite and $f \in C^\infty(\mathbb{R}^m, \mathbb{R}^m)$. The system is equivariant with respect to the action (2.12) of the Euclidean group $SE(2)$ and satisfies (2.1) with the spaces (see [28],[29])

$$Y = C^2_{\text{unif}}(\mathbb{R}^2, \mathbb{R}^m), \quad X = C^0_{\text{unif}}(\mathbb{R}^2, \mathbb{R}^m). \tag{4.2}$$

It is proved in [20] that this is also true for certain cubic nonlinearities for the uniformly local spaces (compare Example 2.14)

$$Y = H^2_{\text{ul}}(\mathbb{R}^2, \mathbb{R}^m), \quad X = L^2_{\text{ul}}(\mathbb{R}^2, \mathbb{R}^m). \tag{4.3}$$

Formally differentiating the action (2.12) with respect to $\gamma = (\theta, b) \in S^1 \ltimes \mathbb{R}^2$ yields the expression

$$S(v, \theta)\lambda := a(\gamma^{-1})\,[a_\gamma(\gamma)v\lambda] = -v_x \left[\varrho_{\frac{\pi}{2}} x\lambda_1 + \varrho_{-\theta} \begin{pmatrix} \lambda_2 \\ \lambda_3 \end{pmatrix}\right], \tag{4.4}$$

for $\lambda_1 \in S^1$, $\lambda_2, \lambda_3 \in \mathbb{R}$.

This formula can be shown rigorously and Hypothesis 2.4 is satisfied if the function v lies in the space

$$\tilde{Y} = \{v \in Y : Pv \in X\},$$

where

$$(Pv)(x) = v_x(x)\varrho_{\frac{\pi}{2}} x = -x_2 v_{x_1} + x_1 v_{x_2}. \tag{4.5}$$

Note that this follows from Proposition 2.12 since the domain of P corresponds to $D(\lambda_1)$ in (2.37) and since Y is contained in the domain of the other two infinitesimal generators $\frac{\partial}{\partial x_1}$ and $\frac{\partial}{\partial x_2}$.

The system (2.20) is of the form

$$v_t = A\Delta v + f(v) - S(v, \theta)\lambda, \quad v(0) = u_0, \tag{4.6}$$

with $S(v, \theta)$ defined in (4.4) and equation (2.21) reads

$$\theta_t = \lambda_1, \quad b_t = \begin{pmatrix} \lambda_2 \\ \lambda_3 \end{pmatrix}, \quad \theta(0) = 0, \quad b(0) = 0. \tag{4.7}$$

In contrast to (3.15) the forcing term on the right hand side of (4.6) depends on the group variable θ. We can eliminate this dependence by choosing new coordinates (θ, α) on G and μ on $\mathcal{A}$ as follows:

$$\alpha = \varrho_{-\theta} b, \quad \mu_1 = \lambda_1, \quad \begin{pmatrix} \mu_2 \\ \mu_3 \end{pmatrix} = \varrho_{-\theta} \begin{pmatrix} \lambda_2 \\ \lambda_3 \end{pmatrix}.$$

This transforms (4.6),(4.7) into

$$v_t = A\Delta v + f(v) - S(v)\mu, \quad v(0) = u_0, \quad S(v)\mu = -v_x \left[\varrho_{\frac{\pi}{2}} x\mu_1 + \begin{pmatrix} \mu_2 \\ \mu_3 \end{pmatrix}\right], \tag{4.8}$$

$$\theta_t = \mu_1, \quad \alpha_t = \mu_1 \varrho_{\frac{\pi}{2}} \alpha + \begin{pmatrix} \mu_2 \\ \mu_3 \end{pmatrix}, \quad \theta(0) = 0, \quad \alpha(0) = 0. \tag{4.9}$$

Note that the second equation in (4.9) is no longer trivial, but describes, in case of constant μ, a rotation on a circle of radius $|\mu_1|$ about the center $\frac{1}{\mu_1}\begin{pmatrix} -\mu_3 \\ \mu_2 \end{pmatrix}$. In this version the two phase conditions (2.33) and (2.35) coincide.

Both systems (4.6) and (4.8) introduce a convection term Pv which becomes large on large domains. The numerical discretization will take this into account, see section 4.2 below.

We write system (4.6) in polar coordinates which are particularly well suited for spiral waves. With $w(r,\varphi) = v(r\cos\varphi, r\sin\varphi)$ we obtain

$$w_t = A\Delta_{r,\varphi} w + f(w) + \lambda_1 w_\varphi + \begin{pmatrix} w_r & \frac{1}{r} w_\varphi \end{pmatrix} \varrho_{-\varphi-\theta} \begin{pmatrix} \lambda_2 \\ \lambda_3 \end{pmatrix} \tag{4.10}$$

with the Laplacian $\Delta_{r,\varphi} w = w_{rr} + \frac{1}{r} w_r + \frac{1}{r^2} w_{\varphi\varphi}$. In the numerical experiments below we use a rectangular grid for (4.10) which corresponds to a polar grid for the original equation (4.6). The numerical experiments show that the influence of the geometry of the domain is much stronger for the frozen system. Using a cartesian grid on a rectangular domain shows strong negative effects of the boundary. In particular, we were not able to freeze non localized spirals in this situation.

An appropriate inner product that is continuous with respect to the topology of the space X in both cases (4.2),(4.3) (compare section 2.3) is

$$\langle u, v \rangle_\eta = \int_{\mathbb{R}^2} u(x)^T v(x) \eta(x) dx, \tag{4.11}$$

where the weight function satisfies (see Example 2.14)

$$\eta \in C^1(\mathbb{R}^2, (0,\infty)) \cap L^1(\mathbb{R}^2), \quad |\nabla \eta(x)| \le C\eta(x), \quad x \in \mathbb{R}^2. \tag{4.12}$$

In some numerical examples below the choice of inner product actually makes a difference because it enters into the phase condition.

4.2. Numerical method. We consider the polar system (4.10) on a rectangle $[0,R] \times [0, 2\pi)$ and use periodic boundary conditions in the φ-direction and Neumann boundary conditions $v_r = 0$ at $r = R$. So far we have not yet set up appropriate projection boundary conditions that generalize the one dimensional case (3.22). These will require to solve a linearized exterior boundary value problem and is expected to be quite expensive. Note that in [9] a simple type of mixed boundary conditions is proposed in order to create spiral solutions for a scalar equation.

For the discretization we choose a rectangular grid on $[0,R]\times[0,2\pi)$ with step-sizes Δr and $\Delta\varphi$. Second order derivatives v_{rr} and $v_{\varphi\varphi}$ are replaced by centered difference quotients; at the origin we use the standard cartesian five-point formula. For the examples in 4.3.1, 4.3.2 below we also use centered differences for the first derivatives. However, for the last example the artificial convection introduced in (4.10) dominates diffusion so that it was necessary to use an upwind-downwind scheme (see 4.3.3 for details) Time is again discretized by a half-explicit Euler method as in (3.18)-(3.20) with $S_{\Delta x}(v^n)\lambda^{n+1}$ replaced by the corresponding discretization of the forcing terms in (4.10). Stability restrictions caused by the use of the half-explicit method

$$\Delta t \le C \min\{(\Delta r)^2, (\Delta\varphi)^2\}$$

are taken into account. Finally, integrals are replaced by trapezoidal sums.

4.3. Examples. The following computations are performed with a version of Barkley's code `ezspiral` [1] that has been adapted to the discretization described in the previous section. In all examples we used the phase condition $\psi_{\min}$ from (2.33) which minimizes the temporal change of v. In fact, the numerical values showed no substantial difference between $\psi_{\min}$ and the phase condition ψ_{orth} from (2.35) which guarantees orthogonality of time and group orbit.

As a general remark concerning all of our computations we note that the λ-values after one time step jump to a consistent value $\lambda = \lambda^1$ according to the algebraic condition (3.20). This is the normal behavior for DAE's and our λ-plots start after this first step.

Movies are linked to some of the figures for better illustration, their color code is identical to the code used in the corresponding figures. The time development of the λ variables is shown in an extra diagram and the behavior of the group variables θ and b is indicated by a black bar and a white trace.

4.3.1. λ-ω-system. Our first example is a $\lambda-\omega$ system [18] in the complex form

$$u_t = \Delta u + (\lambda(|u|) + i\omega(|u|))u, \quad u(x,t) \in \mathbb{C} \tag{4.13}$$

where λ and ω are functions of $|u|$. We take $\lambda(|u|) = 1 - |u|^2$, $\omega(|u|) = -|u|^2$ for which rigidly rotating waves are known to exist [18]. As shown in section 4.1 equation (4.13) is equivariant with respect to the action of the group $SE(2)$ defined in (2.12). We solve the frozen system (4.10),(4.7) together with the phase condition defined by $\psi_{\min}$ using the L^2 inner product. The numerical parameters are $R = 50$, $\Delta r = 0.5$, $\Delta\varphi = \frac{\pi}{40}$, $\Delta t = 1.5421 \cdot 10^{-4}$. Starting from the initial function

$$u_0(r,\varphi) = \tfrac{r}{R}(\cos(\varphi) + i\sin(\varphi)) \tag{4.14}$$

a counter-clockwise rotating spiral develops.

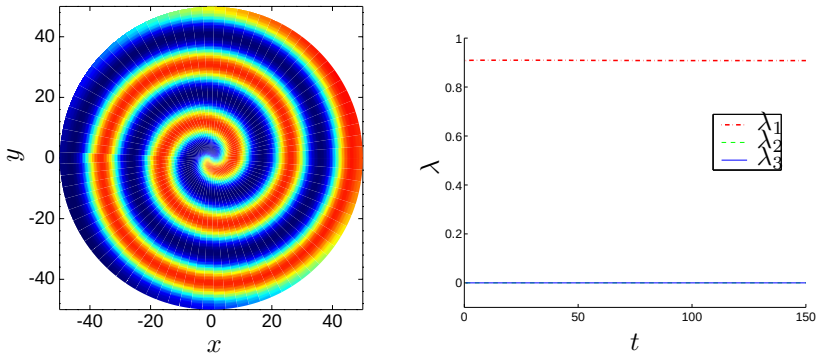

(a) Spiral solution

(b) Evolution of $\lambda(t)$

FIG. 4.1. *$\lambda - \omega$-system.*

In Figure 4.1(a) a color scale plot of a snapshot of the real part of the spiral solution is shown at a fixed time instance.

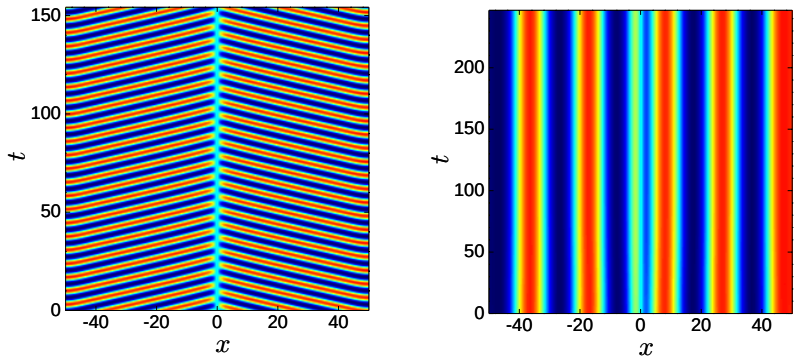

(a) Rotating spiral (b) Frozen spiral

FIG. 4.2. *Time evolution of a slice for the rotating and the frozen spiral for the $\lambda-\omega$-system. Clicking on the movie shows the corresponding animation.*

In Figure 4.2 the time evolution of a slice along the x-axis of the spiral is compared for the rotating and the frozen system. As initial condition we chose the centered spiral shown in Figure 4.1. Figure 4.1(b) shows the corresponding evolution of the λ parameters of the frozen system. The rotational velocity λ_1 instantly jumps to a fixed value of $\bar{\lambda} \approx 0.9$, while the translational speeds λ_2 and λ_3 stay at zero.

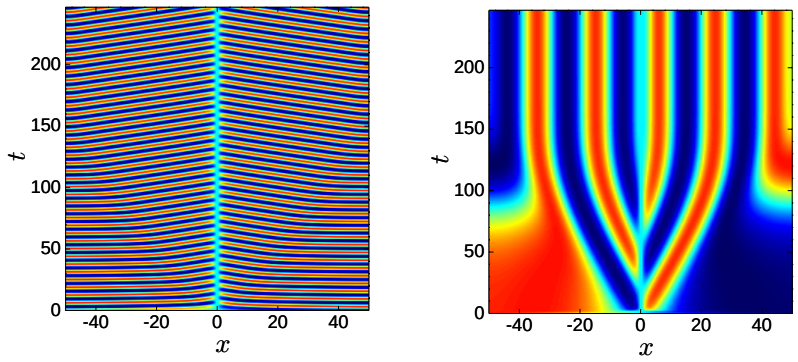

(a) Rotating spiral (b) Frozen spiral

FIG. 4.3. *Time evolution of a slice for the $\lambda-\omega$-system started far away from the spiral wave. Clicking on the movie shows the corresponding animation.*

Figure 4.3 compares the time evolution for the frozen and the non-frozen system starting at the initial value u_0 defined in (4.14) far away from relative equilibria. In both cases eventually a spiral of the same shape develops (faster for the rotating wave than for the frozen wave).

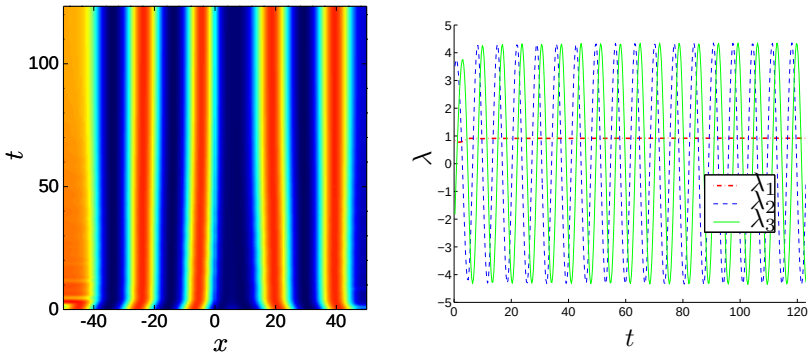

(a) Frozen spiral (b) Evolution of $\lambda(t)$

FIG. 4.4. *$\lambda-\omega$-system started with a shifted spiral, $G = SE(2)$.*

If we start with a slightly shifted spiral we get the results shown in Figure 4.4. Near the boundary the spiral broadens slightly, an effect that decreases with growing size of the domain. The (λ_2, λ_3)-variables in 4.4(b) show that the center of the spiral now rotates on a circle.

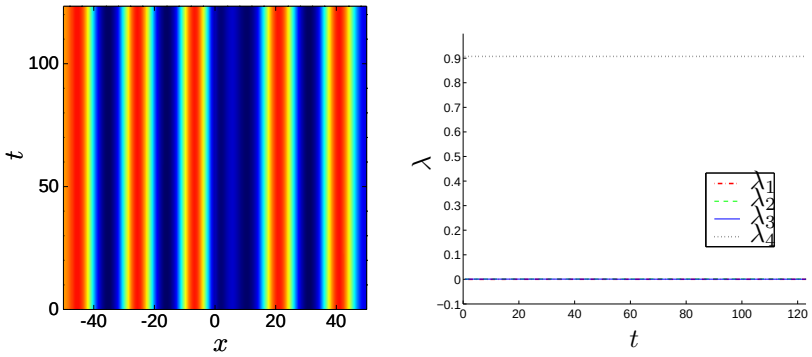

(a) Frozen spiral (b) Evolution of $\lambda(t)$

FIG. 4.5. *$\lambda-\omega$-system started with a shifted spiral, $G = SE(2) \times S^1$.*
Clicking on the movie compares the evolution of the frozen system for both groups, the ϕ variable is indicated by a white bar.

In fact the system (4.13) shows equivariance with respect to the larger group $SE(2) \times S^1$. Denoting group elements by $\gamma = (\theta, b, \phi) \in (S^1 \ltimes \mathbb{R}^2) \times S^1$ the action on

real valued functions and the forcing term in (2.31) are given by

$$\begin{aligned}[a(\gamma)v](x) &= \varrho_{-\phi} v(\varrho_{-\theta}(x-b)),\\ S(v,\gamma)\lambda &= -v_x\left[\varrho_{\frac{\pi}{2}} x\lambda_1 + \varrho_{-\theta}\begin{pmatrix}\lambda_2\\ \lambda_3\end{pmatrix}\right] - \varrho_{\frac{\pi}{2}} v\ \lambda_4.\end{aligned} \tag{4.15}$$

In polar coordinates this leads to the term

$$S(w,\gamma)\lambda = -\lambda_1 w_\varphi - \begin{pmatrix} w_r & \frac{1}{r}w_\varphi\end{pmatrix} \varrho_{-\varphi-\theta}\begin{pmatrix}\lambda_2\\ \lambda_3\end{pmatrix} - \varrho_{\frac{\pi}{2}} w\ \lambda_4.$$

Using the full symmetry group $SE(2)\times S^1$ immediately freezes the spiral wave in the shifted position. Also the velocities $\lambda_1 = \dot\theta$, $(\lambda_2,\lambda_3) = \dot b$, $\lambda_4 = \dot\phi$ stabilize at the stationary values $\bar\lambda_1, \bar\lambda_2, \bar\lambda_3 \approx 10^{-3}$, $\bar\lambda_4 > 0$ (see Figure 4.5) and there are no boundary effects as for $G = SE(2)$ above.

It seems surprising that the smaller group $G = SE(2)$ is sufficient to freeze this spiral wave as shown in Figure 4.4. The reason is as follows: The relative equilibrium $u(x,t)$ has a special symmetry $u(\varrho_\theta x, t) = e^{i\theta}u(x,t)$ (i.e. the stabilizer is nontrivial). This makes it possible to transfer a rotation in the image of u to a rotation in the argument. The slight differences between Figures 4.4(a) and 4.5(a) seem to result from the fact that the coefficient λ_1 of the convective term w_φ in (4.10) is very small for the larger group whereas it is of order one for the smaller group.

4.3.2. Quintic Ginzburg-Landau system. The quintic Ginzburg Landau system (QGL) given by

$$u_t = (\beta + \frac{i}{2})\Delta u - \delta u + (\epsilon + i)|u|^2 u - (\mu + i\nu)|u|^4 u, \quad u(x,t)\in\mathbb{C}$$

posseses strongly localized solutions, so called spinning solitons. These occur at parameter values $\beta = \delta = \frac{1}{2}$, $\epsilon = 2.5$, $\mu = 1$, $\nu = 0.1$, see [7],[8]. The symmetry group is again the four dimensional group $SE(2)\times S^1$, cf. (4.15). We choose the following numerical parameters $R = 20$, $\Delta r = \frac{1}{6}$, $\Delta\varphi = \frac{\pi}{40}$, $\Delta t = 0.771\cdot 10^{-4}$. We start at an initial profile that is obtained by shifting $u_0(r,\varphi) = 0.2\ e^{i\varphi} r e^{-(\frac{r}{7})^2}$ slightly to the right on the x-axis. Then a localized vortex solution develops the real part of which is displayed in Figure 4.6.

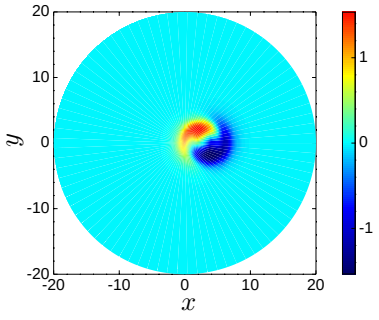

FIG. 4.6. *Quintic Ginzburg-Landau system.*

We take this solution as initial data for the comparison of the rotating wave and its frozen counterpart. Figure 4.7 shows the corresponding time evolution of a slice

along the x-axis. The behavior of the λ parameters for the frozen system is displayed in Figure 4.8(a).

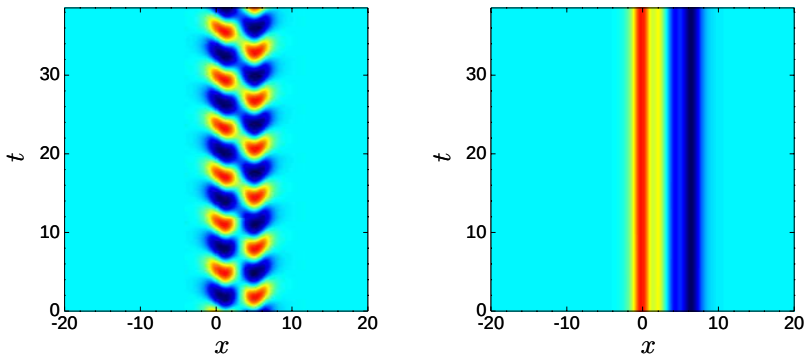

(a) Rotating spiral (b) Frozen spiral

FIG. 4.7. *Time evolution of a slice for the rotating and the frozen vortex for the QGL-system. Clicking on the movie shows the corresponding animation of the original and the frozen system in the transformed variables (see Fig. 4.8(b)).*

Their asymptotic behavior is better revealed by solving the reparametrized equation (4.8), (4.9) (see Figure 4.8(b)). While the v-part is identical for both systems the time plot of the parameters λ and μ shows a clear difference (see Figure 4.8). The values μ_2, μ_3 for the system (4.8),(4.9) stabilize after some time showing that the center of rotation in (4.9) becomes constant. In contrast, the values λ_2, λ_3 for (4.6),(4.7) rotate according to $\binom{\lambda_2}{\lambda_3} = \varrho_\theta \binom{\mu_2}{\mu_3}$. The initial phase of this rotation is shown in Figure 4.8(a). The rotational velocities λ_1, μ_1 and λ_4, μ_4 are identical and rapidly stabilize at specific negative values.

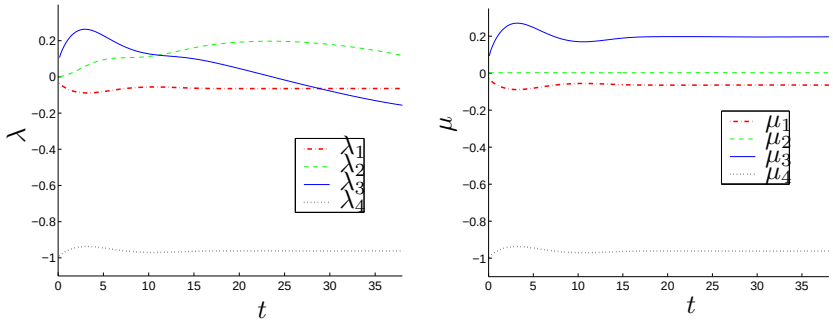

(a) Non-transformed system (b) Transformed system

FIG. 4.8. *Frozen Quintic Ginzburg-Landau system, evolution of parameters.*

Even for an initial value far away from any relative equilibrium the longtime

behavior of the frozen system and the non-frozen system is similar. To this end we compare in Figure 4.9 the time evolution of both systems started with the shifted initial profile mentioned before. This initial function leads to a rotating vortex for the non frozen (see [7]), as well as for the frozen system.

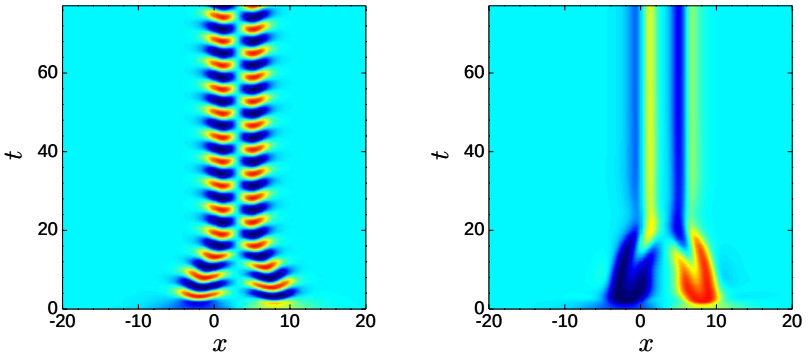

(a) Rotating spiral (b) Frozen spiral

FIG. 4.9. *Time evolution of a slice for the QGL-system with initial data u_0 shifted to the right. Clicking on the movie shows the corresponding animation of the original and the frozen system in the transformed variables.*

4.3.3. Barkley's spiral system. Barkley's well known system [3] is given by

$$u_t = \Delta u + \frac{1}{\epsilon} u(1-u)(u - \frac{v+b}{a})$$
$$v_t = u - v.$$

The equation is equivariant with respect to the action of $SE(2)$, cf. (2.12),(4.4).

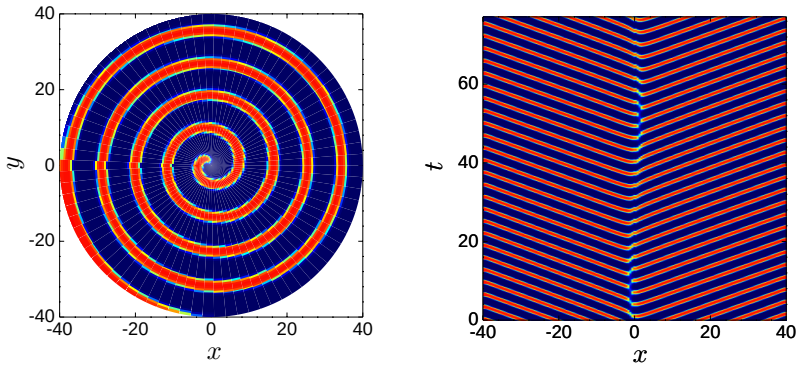

(a) Spiral solution (b) Time evolution of a slice

FIG. 4.10. *Barkley system.*

We test our method in the parameter regime of rigidly rotating waves with $\epsilon = \frac{1}{50}$ and $a = 0.75, b = 0.01$. The numerical parameters are $R = 40$, $\Delta r = 0.5$, $\Delta\varphi = \frac{\pi}{40}$, $\Delta t = 1.5421 \cdot 10^{-4}$.

In Figure 4.10(a) we show a snapshot of the u component of the spiral solution and in Figure 4.10(b) the time evolution of a slice through u along the x-axis is displayed.

Since the system is of mixed hyperbolic-parabolic type, discretizing the convective terms with an upwind/downwind scheme becomes essential. In the previous examples diffusion was strong enough to dominate convection introduced by the freezing procedure. For this example the contributions to first order derivatives are assembled in $b_1(r,\varphi)w_r$ resp. $b_2(r,\varphi)w_\varphi$ and approximated by

$$b_j(r,\varphi)D_\pm w = b_j(r,\varphi)[\chi(b_j(r,\varphi))D_+ w + (1-\chi(b_j(r,\varphi)))D_- w], \quad j = 1,2.$$

The symbols D_+,D_- denote forward and backward difference quotients in the r or φ direction and the switching function χ is defined by

$$\chi(b) = (1+\exp(-\beta\, b))^{-1}, \quad \beta = 0.2.$$

The value of β has been chosen in order to balance oscillations introduced by using centered diffences for the convective terms ($\beta = 0$) and artificial diffusion introduced by a strict switching rule (β large).

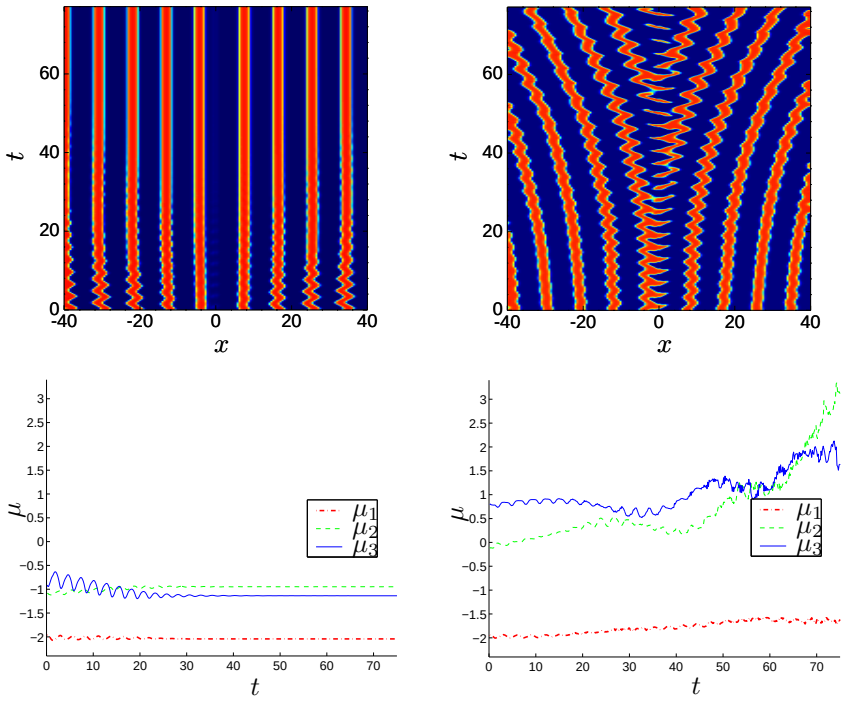

(a) L^2_η phase condition
The linked movie compares the rotating and the frozen system.

(b) L^2 phase condition
The linked movie compares the weighted and the non weighted system.

FIG. 4.11. *Frozen Barkley system, time evolution of a slice and of parameters μ.*

We start at a spiral wave which rigidly rotates in the non-frozen case. As Figure 4.10(b) shows, the spiral core still exhibits a slight oscillatory motion.

Figure 4.11(a) shows the result for the frozen system with a weighted L^2 norm, where the weight in equation (4.11) is $\eta(x) = e^{-0.5|x|}$. After some small initial oscillations the wave eventually freezes and the parameters μ of the transformed system stabilize.

The importance of the weight in the phase condition is demonstrated in Figure 4.11(b) which shows the results for the L^2 inner product without weight. Now the spiral is perturbed by an oscillatory motion of the spiral core and finally drifts out of the region. The corresponding μ variables oscillate and drift away as well. These results suggest that the use of the weighted inner product for the phase condition keeps the continous spectrum in the left half plane while the L^2 inner product destabilizes the spectrum. Stabilization by the phase condition only, seems to be different from shifting the whole spectrum to the left by considering the differential equation in a weighted function space as in [27]. The details of this mechanism need further investigation.

Initial values that are far away from relative equilibria, lead to large differences of the time evolution for the frozen and the non-frozen system. While the non-frozen system develops a rigidly rotating spiral, we were not able to stabilize a corresponding frozen solution in a large time interval.

In summary, it turns out that freezing the spiral in Barkley's system is much more sensitive than in the previous examples. This is probably due to the mixed hyperbolic-parabolic type of the equation which requires more sophisticated numerical methods than our simple half-explicit scheme. Moreover, it seems quite a challenging task to freeze drifting spirals or recognize meandering spirals as periodic orbits.

Acknowledgements. The authors thank both referees for their useful suggestions which considerably helped in improving the first version of the paper.

REFERENCES

[1] D. Barkley. A model for fast computer simulation of waves in excitable media. *Physica D*, 49:61–70, 1991.

[2] D. Barkley. Linear stability analysis of rotating spiral waves in excitable media. *Phys. Rev. Lett.*, 68:2090–2093, 1992.

[3] D. Barkley. Euclidean symmetry and the dynamics of rotating spiral waves. *Phys. Rev. Lett.*, 72:164–167, 1994.

[4] W.-J. Beyn. The numerical computation of connecting orbits in dynamical systems. *IMA J. Numer. Anal.*, 10(3):379–405, 1990.

[5] V. N. Biktashev, A. V. Holden, and E. V. Nikolaev. Spiral wave meander and symmetry of the plane. *Internat. J. Bifur. Chaos Appl. Sci. Engrg.*, 6(12A):2433–2440, 1996.

[6] P. Chossat and R. Lauterbach. *Methods in Equivariant Bifurcations and Dynamical Systems*. World Scientific, 2000.

[7] L.-C. Crasovan, B. A. Malomed, and D. Mihalache. Stable vortex solitons in two-dimensional ginzburg-landau equation. *Physical Review E*, 63, 2000.

[8] L.-C. Crasovan, B. A. Malomed, and D. Mihalache. Spinning solitons in cubic-quintic nonlinear media. *Pramana Journa of Physics*, 57(5/6):1041–1059, 2001.

[9] M. Dellnitz, M. Golubitsky, A. Hohmann, and I. Stewart. Spirals in scalar reaction diffusion equations. *Int. J. Bif. Chaos Appl. Sci. Engrg.*, 5:1487–1501, 1995.

[10] B. Fiedler, B. Sandstede, A. Scheel, and C. Wulff. Bifurcations from relative equilibria of noncompact group actions: skew products, meanders and drifts. *Doc. Math. J. DMV*, 1:479–505, 1996.

[11] B. Fiedler and D. Turaev. Normal forms, resonances, and meandering tip motions near relative equilibria of Euclidean group actions. *Arch. Ration. Mech. Anal.*, 145(2):129–159, 1998.

[12] M. Field. Symmetry breaking for compact Lie groups. *Mem. Amer. Math. Soc.*, 120(574):viii+170, 1996.
[13] M. Golubitsky, V. G. LeBlanc, and I. Melbourne. Meandering of the spiral tip: an alternative approach. *J. Nonlinear Sci.*, 7(6):557–586, 1997.
[14] W. J. F. Govaerts. *Numerical methods for bifurcations of dynamical equilibria*. Society for Industrial and Applied Mathematics (SIAM), Philadelphia, PA, 2000.
[15] E. Hairer, C. Lubich, and M. Roche. *The numerical solution of differential-algebraic systems by Runge-Kutta methods*, volume 1409 of *Lecture Notes in Mathematics*. Springer-Verlag, Berlin, 1989.
[16] E. Hairer and G. Wanner. *Solving ordinary differential equations. II*, volume 14 of *Springer Series in Computational Mathematics*. Springer-Verlag, Berlin, second edition, 1996. Stiff and differential-algebraic problems.
[17] D. Henry. *Geometric Theory of Semilinear Parabolic Equations*. Number 804 in Lecture Notes in Mathematics. Springer, 1981.
[18] Y. Kuramoto and S. Koga. Turbulized rotating chemical wavies. *Progress of Theoretical Physics*, 66(3):1081–1085, 1981.
[19] A. Mielke. The Ginzburg-Landau equation in its role as a modulation equation. In B. Fiedler, editor, *Handbook of Dynamical Systems*, volume II, pages 759–834. Elsevier, 2002.
[20] A. Mielke and G. Schneider. Attractors for modulation equations on unbounded domains - existence and comparison. *Nonlinearity*, 8:743–768, 1995.
[21] R. M. Miura. Accurate computation of the stable solitary wave for the FitzHugh–Nagumo equations. *J. Math. Biology*, 13:247–269, 1982.
[22] J. D. Murray. *Mathematical Biology*. Springer, 1989.
[23] E. V. Nikolaev, V. N. Biktashev, and A. V. Holden. On bifurcations of spiral waves in the plane. *Internat. J. Bifur. Chaos Appl. Sci. Engrg.*, 9(8):1501–1516, 1999.
[24] C. W. Rowley, I. G. Kevrekidis, J. E. Marsden, and K. Lust. Reduction and reconstruction for self-similar dynamical systems. *Nonlinearity*, 16:1257–1275, 2003.
[25] C. W. Rowley and J. E. Marsden. Reconstruction equations and the Karhunen-Loève expansion for systems with symmetry. *Physica D*, 142:1–19, 2000.
[26] B. Sandstede. Convergence estimates for the numerical approximation of homoclinic solutions. *IMA J. Numer. Anal.*, 17(3):437–462, 1997.
[27] B. Sandstede and A. Scheel. Absolute versus convective instability of spiral waves. *Phys. Rev. E (3)*, 62(6, part A):7708–7714, 2000.
[28] B. Sandstede, A. Scheel, and C. Wulff. Dynamics of spiral waves on unbounded domains using center-manifold reductions. *J. Diff. Eqns.*, 141:122–149, 1997.
[29] B. Sandstede, A. Scheel, and C. Wulff. Bifurcations and dynamics of spiral waves. *J. Nonlinear Sci.*, 9(4):439–478, 1999.